Quenching of excited $^1P_1$ state atomic zinc by molecular nitrogen: A matrix-isolation spectroscopy/quantum chemical calculation study

Fernando Colmenares
Departmento de Fisica y Quimica Teorica, Facultad de Quimica, Universidad Nacional Autonoma de Mexico, Mexico DF 04510, Mexico

John G. McCaffrey
Department of Chemistry, National University of Ireland at Maynooth, Maynooth, Co. Kildare, Ireland

Octavio Novaro[a)]
Instituto de Fisica, Universidad Nacional Autonoma de Mexico, Apartado Postal 20-364 Mexico DF 01000, Mexico

(Received 8 February 2001; accepted 20 March 2001)

A concentration study is used to identify the optical absorption of zinc atoms isolated in solid nitrogen. Photoexcitation of the threefold-split, atomic $4p\,^1P_1$ singlet absorption band did not produce any emission from either the singlet or triplet states. Hartree–Fock (relativistic effective core potentials) plus variational and multireference perturbational configuration-interaction calculations are performed to analyze this very efficient quenching of excited state atomic zinc by molecular nitrogen. Of the two geometries considered in energy calculations of the approach of $Zn(^1P_1)$ to N_2, the collinear exhibited a slightly greater stabilization than the perpendicular approach. However, the collinear is identified as of no significance in the excited state quenching due to the absence of low energy crossings with the ground state. In contrast, for the perpendicular approach a crossing between the repulsive ground $^1A_1(^1S_0)$ state and the strongly attractive $^1B_2(^1P_1)$ state occurs close to the energy minimum of the $^1B_2$ state. The efficiency of crossing between these states is analyzed in the framework of one-dimensional Landau–Zener (LZ) theory. A hopping probability of 0.07 is obtained for a single crossing, considered important in a rapidly relaxing solid state system, such as present in a low temperature matrix. Crossings found between the repulsive $^3B_1(^3P_1)$ and $^3A_1(^3P_1)$ states with the strongly bound $^1B_2(^1P_1)$ state are expected to play a role in gas phase $Zn(^1P_1)$ quenching leading to the production of $Zn(^3P_J)$ states. LZ calculations indicate a small hopping probability for these crossings, consistent with the small $^1P_1 \rightarrow {}^3P_J$ quenching cross sections observed in the gas phase work. © *2001 American Institute of Physics.* [DOI: 10.1063/1.1370952]

I. INTRODUCTION

The efficiency of electronic to vibrational ($E-V$) energy transfer between excited state metal atoms and molecular nitrogen has been examined in quenching studies of the $^3P_1$ state of mercury both under gas phase[1] and matrix-isolation conditions.[2] The result of the $E-V$ transfer process in the matrix system has also been examined by monitoring the relaxation of highly vibrationally excited levels (up to $v=17$) of the N_2 molecule in FTIR emission spectroscopy.[3] *Ab initio* calculations[4] have also been carried out on the $Hg(^3P_1)/N_2$ system highlighting the role of bound excited states in the $E-V$ transfer process.

In contrast to the Hg system, fewer works have appeared in the literature on the gas phase quenching of atomic zinc by nitrogen. Krause and co-workers[5] recorded a total cross section of 26 Å^2 for quenching of $Zn(^1P_1)$ by N_2, with a relative cross section for the formation of $Zn(^3P_J)$ of about 6 Å^2. This singlet quenching cross section is in accordance with earlier work by Breckenridge and Renlund[6] in which a value of 19 Å^2 was recorded. The small relative cross section indicates that $Zn(^3P_J)$ is formed in small yield, with formation of $Zn(^1S_0)$ the dominant channel. A considerably smaller cross section of 0.6 Å^2 has been measured by Umemoto and co-workers[7] for the $Zn(^3P_1)/N_2$ system indicating that nitrogen quenching of the triplet state of zinc is much less efficient than the singlet state.

Although the first matrix absorption spectra of atomic zinc were published[8–10] many years ago using the solid rare gases as hosts, no literature appears to exist for solid nitrogen as a host. Indeed, it is only quite recently that the luminescence spectroscopy of matrix-isolated atomic zinc has been reported[11] by the Maynooth Group. The efficiency of molecular nitrogen quenching became evident in our work on the luminescence spectroscopy of matrix-isolated atomic zinc, in which it was found that even minor atmospheric leaks in the gas handling system were sufficient to completely quench the singlet emission of atomic zinc. This is probably the reason for the report[12] of several years ago, that atomic $^1P_1$ zinc does not emit in rare gas matrices which were known from absorption spectra, to contain zinc atoms.

The matrix luminescence spectroscopy of atomic zinc

[a)]Member of El Colegio Nacional.

can be summarized as consisting of pairs of emission bands with the efficiency of singlet emission very high in solid argon and totally quenched in solid xenon. In solid xenon intense triplet emission is produced in very high yield following singlet excitation. An understanding of the matrix luminescence was facilitated by the large body of complementary data available on the interaction potentials of diatomic zinc atom/rare gas atom van der Waals species (Zn·RG). These species have been generated in supersonic expansions by Breckenridge and co-workers[13–17] and Umemoto *et al.*[18] and their ''pair-potentials'' have been used in well established[19] theoretical models[20] to simulate metal atom spectroscopy in the solid rare gases. Spectral simulations based on pair-potentials has allowed identification of the pairs of the emission bands present in the solid rare gases as due to two distinct vibronic modes coupling in the excited state. Moreover, the pair-potentials work has facilitated an assignment of the enhanced ISC process of atomic zinc in the heavier rare gases as due to a curve crossing mechanism[21] between a strongly attractive singlet state and a repulsive triplet state.

In this contribution we present the results of a concentration study made with absorption spectroscopy for the isolation of atomic zinc in solid nitrogen and our attempts to record luminescence following excitation to the $4s4p\ ^1P_1$ state. In the remainder, the bulk of the paper, we present the results of quantum chemical calculations for the interaction of ground and excited state atomic zinc with molecular nitrogen in both end-on and side-on approaches. Finally, from the crossings identified in *ab initio* potential energy curves, a one-dimensional Landau Zener model is used to calculate surface hopping probabilities.

II. METHODS

A. Experiment

Thin film Zn/N_2 samples were prepared by the condensation of nitrogen gas and zinc vapor, onto a lithium fluoride (LiF) window mounted on the cold tip of a Leybold continuous flow UHV liquid helium cryostat. Zinc vapor was produced by electron bombardment of 0.25 mm thickness zinc foil (Goodfellow 99.9% purity) coiled into a 5 mm diam molybdenum crucible, positioned in an Omicron EFM3 UHV evaporator. Metal vaporisation rates were recorded with a flux monitor mounted in the EFM3. A deposition temperature of 12 K was found optimal for obtaining samples with good optical characteristics containing a minimum of zinc atoms in multiple trapping sites. The UHV sample chamber was pumped continuously with a Pfeiffer/Balzers TPU 240 turbomolecular pump. Prior to, but not during deposition, a CTI Cryogenics ''Cryo-Torr'' high vacuum pump was used to improve the vacuum still further. Vacuum on the order of 10^{-9} mbar was achieved prior to cool-down, dropping to 10^{-10} mbar after cooldown, was monitored with an HPS Division/MKS Series 423 I-Mag cold-cathode gauge. Gas flow rates were controlled by an Oxford Applied Research piezoelectric PLV 3000 valve and were generally in the range of 3.5–5 mmol/h for periods of between 30–45 min.

Optical measurements were conducted as described in previous publications[11] at the HIGITI experimental station in HASYLAB at DESY, Hamburg using synchrotron radiation (SR) optimized in the VUV spectral region from the W3 beamline. Absorption spectra were recorded in the region of the first resonance $4s4p\ ^1P_1 \leftarrow 4s^2\ ^1S_0$ transition of atomic zinc occurring at 213.9 nm in the gas phase,[22] by scanning with a 1 m normal-incidence, modified Wadsworth monochromator. Absorption spectra were calculated by using pure nitrogen samples, prepared under identical conditions as those containing zinc, as blanks.

B. Computation

All the $Zn+N_2$ interactions reported in this study were calculated at the Hartree–Fock (HF) level using the PSHF code[23] which is a pseudopotential adapted version of the HONDO program. The core electrons were taken into account in accordance with the theory developed by Durand and Barthelat.[24] For the zinc atom, the averaged relativistic effective potential (AREP) and the basis set given by Hurley *et al.*[25] were used. For the valence region, which includes only the $4s$ and $3d$ subshells, the primitive basis was contracted following a $(4s,5d)/[211,311]$ scheme. As excited electronic states involving the $4p$ subshell of the zinc atom were investigated, this triple-ζ quality basis was augmented with two p-type diffuse functions taken from the Wachters[26] tables and scaled by the factor 1.5, as recommended by the author for use in molecular calculations. For consistency, the nitrogen atoms were taken into account using the AREP and the $(5s,5p)/[311,311]$ triple-ζ quality basis set for the $2s$ and $2p$ valence region subshells developed by Pacios and co-workers.[27,28]

MCSCF calculations[29] were carried out on each of the states investigated to determine the optimal molecular orbital set to be used in the MRCI treatment. Calculations beyond the HF level were performed with the CIPSI algorithm[30,31] which allows a variational and a second-order perturbational treatment of the electron correlation. For each electronic state, this electron correlation approach involved a variational reference space of nearly 500 configurations and more than 20 million configurations in the perturbational space.

III. RESULTS

A. Absorption spectroscopy

The isolation of zinc atoms in solid nitrogen follows the behavior previously observed[11] in the solid rare gases. A typical concentration study conducted for deposition of zinc in nitrogen at 12 K is shown in Fig. 1. Exclusive isolation of zinc atoms is observed in the bottom trace where the lowest metal vapor flux has been used. The atomic transition is centered at 210.3 nm—blue shifted by 785 cm^{-1} from the position of the $4p\ ^1P_1 \leftarrow 4s\ ^1S_0$ resonance transition of atomic zinc at 213.86 nm in the gas phase.[22] The atomic bands shown in Fig. 1 show signs of threefold splitting behavior also seen in the solid rare gases. The line shape analysis done of the Zn/N_2 atomic absorption band to resolve these features is presented in Fig. 2. A satisfactory fit was obtained with three gaussian functions centered at 212.42, 210.33, and 208.19 nm each with a width (FWHM) of 760 cm^{-1}. Three-

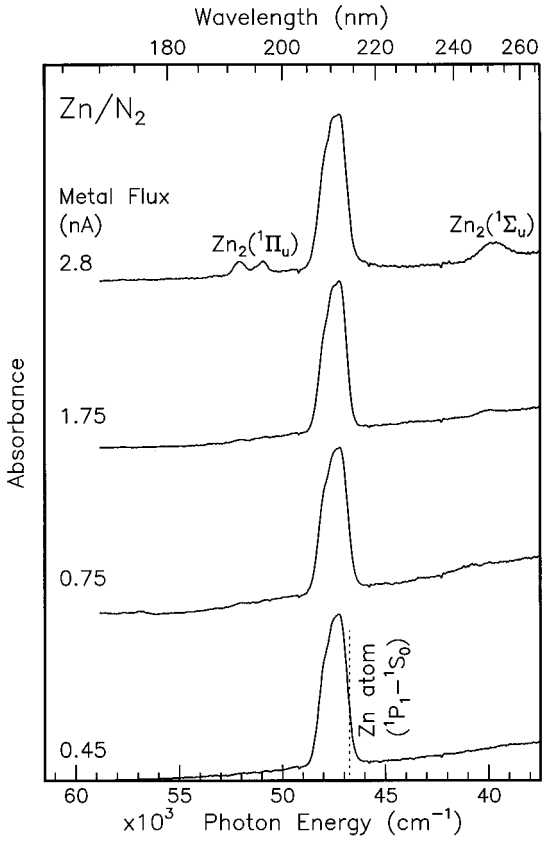

FIG. 1. Absorption spectra recorded at 6 K for matrix samples prepared by the condensation of zinc vapor with nitrogen onto a LiF window at 12 K. The concentration study presented allows the band centered at 210 nm to be assigned to atomic zinc. From the indicated location of the $4s4p\ ^1P_1 \leftarrow 4s^2\ ^1S_0$ transition of atomic zinc in the gas phase, a small blue shift is exhibited in the matrix absorption. The presence of partially resolved three-fold splitting on the atomic transition is noteworthy and analyzed in Fig. 2.

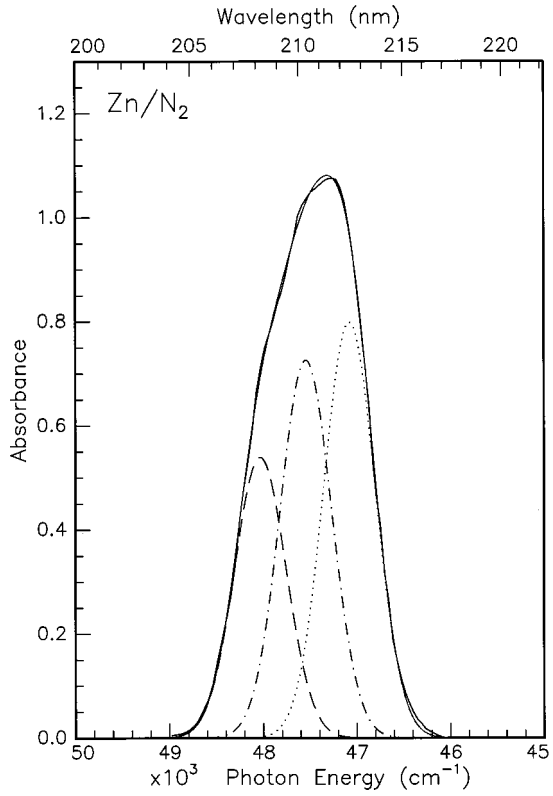

FIG. 2. A line shape analysis of the atomic absorption band recorded in the most dilute Zn/N_2 sample. Three Gaussian functions of equal width (760 cm^{-1} FWHM) centered at 47 067, 47 543, and 48 044 cm^{-1} were extracted in the fit shown. This corresponds to components at 212.42, 210.33, and 208.19 nm.

fold splitting of the atomic transition is indicative of Jahn-Teller interaction in the excited $^1P_1$ state, leading to a removal of the original orbital degeneracy and a lowering of the energy.

Based on the concentration dependence exhibited, the band at 253 nm and the pair of features at 193 and 197 nm, evident in the top trace of Fig. 1, can be assigned to the transitions of zinc dimer. Indeed theoretical calculations[32] indicate that the dimer feature to the red of the atomic band is due to the $A\ ^1\Sigma_u^+ \leftarrow X\ ^1\Sigma_g^+$ transition of Zn_2 while the pair[33] on the blue are due to the $^1\Pi_u^+ \leftarrow X\ ^1\Sigma_g^+$ transition.

B. Emission spectroscopy

In contrast to atomic zinc isolated in the solid rare gases,[11] excitation of the Zn $4s4p\ ^1P_1 \leftarrow 4s^2\ ^1S_0$ transition at 210 nm in a nitrogen matrix produces no detectable emission in the UV-visible spectral region. Careful checks were made in the UV, i.e., in the region immediately to the red of the atomic absorption and in the near-UV (300–400 nm) spectral regions. No emission was observed in either region. Moreover, absorption spectra recorded after prolonged excitation at the $4s4p\ ^1P_1 \leftarrow 4s^2\ ^1S_0$ resonance indicated no change to the spectra recorded on deposition. From these observations it can be stated: (1) that neither singlet nor triplet emission occurs for atomic zinc isolated in solid nitrogen and (2) a photochemical quenching is not occurring. Combining these two statements one must then conclude that a nonradiative process couples the excited state of atomic zinc to the ground state.

To investigate the origin of the quenching of the $4s4p\ ^1P_1$ state of atomic zinc in nitrogen, high level *ab initio* calculations were undertaken for the interaction of excited $Zn(4s4p\ ^1P_1)$ and $Zn(4s4p\ ^3P_J)$ states as well as the ground $Zn(4s^2\ ^1S_0)$ state with molecular nitrogen. Two geometries, collinear ''end-on'' and perpendicular ''side-on,'' were considered for the approach of the zinc atom to molecular nitrogen. The theoretical results obtained are outlined ahead, but before analyzing these results it is worthwhile to consider the possible contributions charge transfer interactions make to the binding energy in the excited states of the ZnN_2 system.

The energetics of the resulting ions indicate that the lowest energy excited state involves transfer of charge from zinc to nitrogen. A Mulliken population analysis presented ahead, verifies this prediction which can be rationalised when one considers that the ionization potential (IP) of atomic zinc is 9.3942 eV while that of N_2 is 15.581 eV. The attractive part of the excited state potentials, arising from the electrostatic interaction between the Zn^+ and N_2^- ions, can be represented by the following equation:

$$V(r)=E_{\infty}-\frac{e^2}{r}, \tag{1}$$

in which $E_{\infty}=\mathrm{IP}(\mathrm{Zn}\,^1P_1)-\mathrm{EA}(\mathrm{N_2})$ is the asymptotic energy of the ion pair. E_{∞} has a value of 5.498 eV, if the electron affinity of molecular nitrogen is taken to be -1.9 eV and $\mathrm{IP}(\mathrm{Zn}\,^1P_1)$ is 3.598 eV. The crossing point of the neutral $\mathrm{Zn}(^1P_1)+\mathrm{N_2}$ and the ''ionic'' $\mathrm{Zn}^+ + \mathrm{N_2}^-$ curves occurs at 2.62 Å if it is assumed the neutral curve is flat.

C. Theoretical calculations

1. Potential energy surfaces

Potential energy surfaces were calculated for all the electronic states of the $\mathrm{ZnN_2}$ molecule belonging to the side-on (C_{2v}) and end-on ($C_{\infty v}$) coordination modes that evolve from the ground state, $\mathrm{Zn}(^1S)+\mathrm{N_2}$, and the first two excited states, $\mathrm{Zn}(^3P)+\mathrm{N_2}$ and $\mathrm{Zn}(^1P)+\mathrm{N_2}$. For each state, we have first studied the interaction of the zinc atom with the nitrogen molecule, keeping the N–N distance fixed at the equilibrium value of the isolated $\mathrm{N_2}$ molecule. For the attractive states detected in this way, relaxation of the N–N distance was allowed. For electronic states belonging to the C_{2v} symmetry point group, the Zn–N distance was optimized for each N–Zn–N angle. For the linear states, optimization of the N–N distance was carried out for each Zn–N(1) distance, where N(1) is the nitrogen atom nearest to the metallic center. This N–N distance relaxation procedure was also followed for calculating the potential energy curves corresponding to the $^1A_1$ (side-on) and $^1\Sigma$ (end-on) repulsive states evolving from the ground state dissociation limit, $\mathrm{Zn}(^1S)+\mathrm{N_2}$, as well as those associated with the $^3A_1$ and $^3B_1$ side-on interaction channels which correlate with the first excited state $\mathrm{Zn}(^3P)+\mathrm{N_2}$ of the free fragments. For the remaining repulsive electronic states in both geometries, the N–N distance was held fixed at the equilibrium value of the isolated molecule for the entire intervals shown in the figures.

2. Potential energy surfaces details

a. Side-on approach As shown in Fig. 3, the $^1A_1$ electronic state, which correlates with the ground state $\mathrm{Zn}(^1S)+\mathrm{N_2}$ dissociation limit, has a repulsive character. Similar behavior is found for all the other electronic states belonging to the A_1 irreducible representation which evolve from the excited $\mathrm{Zn}(^3P)+\mathrm{N_2}$ and $\mathrm{Zn}(^1P)+\mathrm{N_2}$ asymptotes. In fact, only the $^3B_2$ and $^1B_2$ electronic states corresponding to the $\mathrm{Zn}(^3P)+\mathrm{N_2}$ and $\mathrm{Zn}(^1P)+\mathrm{N_2}$ dissociation limits, respectively, are attractive. The corresponding states belonging to the B_1 irreducible representation of this symmetry point group also have a repulsive character. For the attractive $^3B_2$ and $^1B_2$ states, local energy minima were located at roughly the same N–N distance of 2.3455 a.u. and for an N–Zn–N angle of 35°. Although an appreciable lowering of the energy is achieved through the $^3B_2$ and $^1B_2$ reaction channels, with respect to the energy of the corresponding excited state dissociation limits, $\mathrm{Zn}(^3P)+\mathrm{N_2}$ and $\mathrm{Zn}(^1P)+\mathrm{N_2}$, respectively, both energy minima lie above the ground state energy of the free fragments. The triplet state energy lies 0.128 66 a.u. above the ground state dissociation limit energy, whereas the singlet state energy is 0.140 67 a.u. In accord with the geometry parameters mentioned above for these energy minima, an increase of the N–N distance of approximately 13% is found with respect to the equilibrium distance of the isolated molecule.

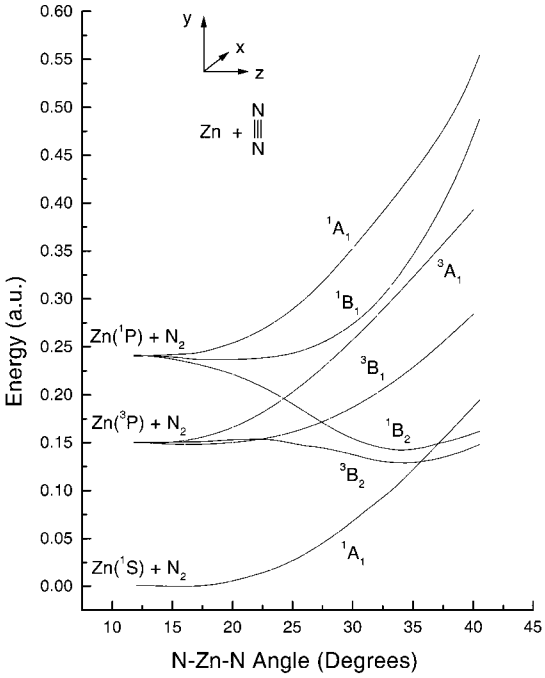

FIG. 3. Calculated energies of the ground and first two excited states of the $\mathrm{Zn}\cdot\mathrm{N_2}$ system for the perpendicular, side-on (C_{2v}) approach of atomic zinc to molecular nitrogen.

b. End-on approach Potential energy curves of the molecular states arising in the linear geometry are shown in Fig. 4. All the sigma-type electronic states of the molecule asso-

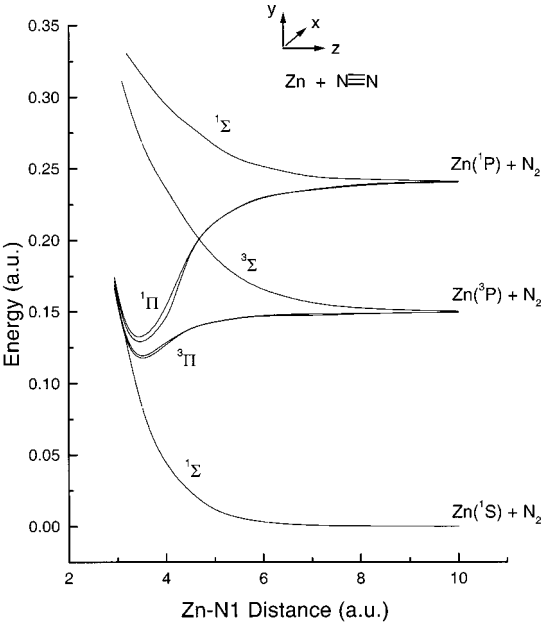

FIG. 4. Calculated ground and first two excited states of the $\mathrm{Zn}\cdot\mathrm{N_2}$ system for the collinear, end-on ($C_{\infty v}$) approach of atomic zinc to molecular nitrogen.

ciated with the ground state and the first two excited states of the free fragments are repulsive. In contrast, the Π-type states evolving from the $Zn(^3P)+N_2$ and $Zn(^1P)+N_2$ asymptotes have an attractive character. Just as for the C_{2v} electronic states mentioned above, the energy minima of the bound Π-states also lie above the energy of the ground state dissociation limit. For the degenerate $^3\Pi_x$ and $^3\Pi_y$ triplet states, a local energy minimum was located at a Zn–N distance of 3.5 a.u. and an N–N distance of 2.268 a.u. (this minimum is 0.1182 a.u. above the ground state energy of the free fragments). In this case, there is an increase of the N–N distance of approximately 10%, with respect to the equilibrium distance of the N_2 isolated molecule. The local energy minima of the degenerate $^1\Pi_x$ and $^1\Pi_y$ singlet states were located at roughly the same Zn–N and N–N distances as those found in the triplet states.

From the results presented above, the two degenerate $^3\Pi_x$ and $^3\Pi_y$ electronic states belonging to the $C_{\infty v}$ symmetry lie at the lowest energy level of the excited ZnN_2 molecule. However, it is worth pointing out that a slightly greater elongation of the N–N distance is associated with the $^3B_2$ and $^1B_2$ electronic states belonging to the C_{2v} symmetry point group, even though these states lie above the lowest energy level of the linear geometry.

3. Surface hopping calculations

As indicated in Figs. 3 and 4, several curve crossings occur between the strongly attractive, excited state $^1B_2(^1\Pi_1)$ curves and the repulsive excited triplet states as well as a single crossing with the repulsive ground state. The importance of these crossings in the excited state quenching of atomic zinc by nitrogen falls into two categories. The first involves a crossing of the spin singlet states, the second involves spin singlet/triplet crossings. Because of the relatively small spin–orbit coupling in atomic zinc, the second category is of less importance in the excited singlet state quenching.

a. Spin singlet crossings Figure 3 reveals that in the perpendicular (C_{2v}) approach, a crossing occurs between the bound, excited singlet state $^1B_2(^1P_1)$ curve and the repulsive ground $^1A_1(^1S_0)$ singlet curve at an N–Zn–N angle of 37.1°—close to the energy minimum of the bound state. In contrast, a low energy crossing[34] does not, as shown in Fig. 4, occur between the bound $^1\Pi(^1P_1)$ state and the repulsive $^1\Sigma(^1S_0)$ curve in the collinear approach. Hence, we conclude that the excited singlet state quenching of atomic zinc by molecular nitrogen at low temperatures occurs predominately for side-on approach of these two species.

To estimate the efficiency of the nonadiabatic singlet $^1B_2/^1A_1$ state crossing, the probability of surface hopping was calculated in the one-dimensional Landau–Zener (LZ) model with the following formula:[35]

$$P_{\mathrm{LZ}}=\exp\left(-\frac{4\pi^2V_{12}^2}{h\nu|F_1-F_2|}\right). \tag{2}$$

In this equation, the matrix element, V_{12}^2, coupling the $^1B_2/^1A_1$ state potentials at their crossing point, r_c, is obtained by calculating their energy splitting in C_s symmetry.

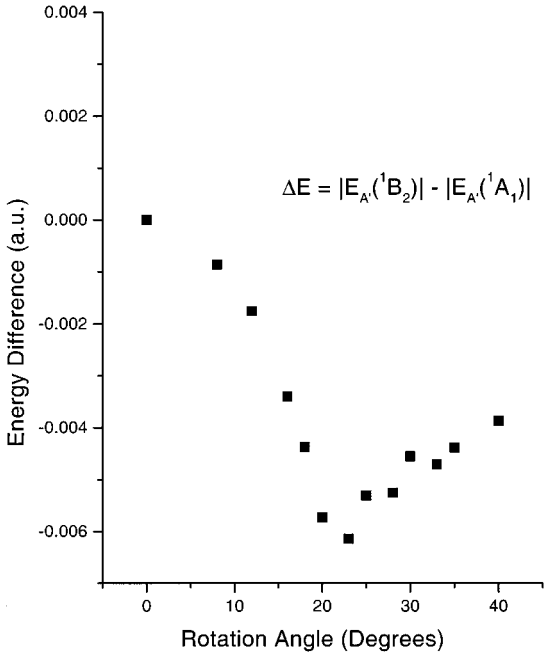

FIG. 5. The magnitude of the curve avoidance induced at the crossing of $^1B_2$ and $^1A_1$ states by the asymmetric stretching mode.

This is achieved, as outlined in Appendix A, by considering the effect of the asymmetric stretching mode at the C_{2v} crossing point. The resulting *ab initio* points are shown in Fig. 5 in which a maximum splitting of 6.314 mhartree was obtained at an angle of 23° away from the T-shape geometry.

In Eq. (2), F_1 and F_2 are the gradients of the $^1B_2$ and the $^1A_1$ diabatic states at their crossing point, r_c. To determine the nuclear velocity term, v, a change in the representation of the approach geometry is made from the angular coordinate shown in Fig. 3 to the center-of-mass distance system shown in Fig. 6. A cubic spline of the *ab initio* data points was then made to identify the crossing point more precisely. The nuclear velocity at the crossing point has been obtained from the expression $v=\sqrt{(2E_{\mathrm{kin}}/\mu)}$ in which μ is the re-

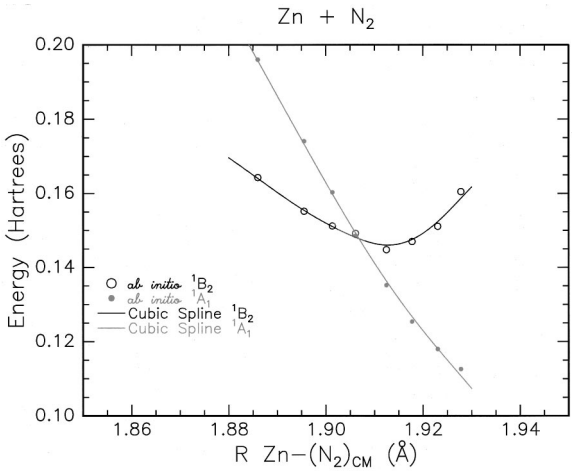

FIG. 6. Details of the curve crossing found between the $^1B_2$ and $^1A_1$ states in the side on approach. The *x*-abscissa shown is zinc to N_2 center-of-mass distance. The filled and open circles are the calculated *ab initio* points, while the solid curves are cubic splines to these points.

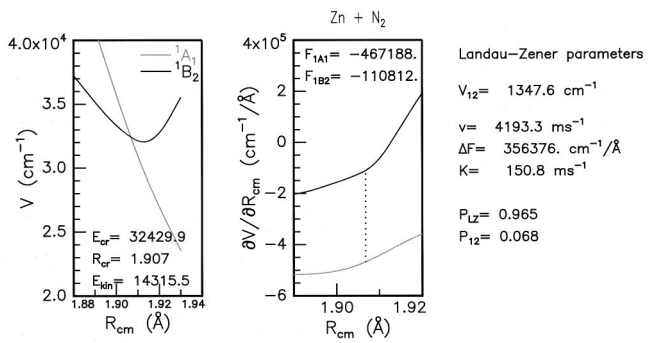

FIG. 7. Parameters involved in the calculation of the LZ hopping probability of the $^1B_2/^1A_1$ crossing in the $Zn\cdot N_2$ system.

duced mass of the $Zn+N_2$ collision pair. E_{kin} is the kinetic energy obtained as the energy difference between the region of the $^1B_2$ state potential accessed in Franck–Condon absorption and the crossing point. The hopping probability, P_{12}, between the two diabatic curves 1 ($V_{1_{A_1}}(R)$) and 2 ($V_{1_{B_2}}V(R)$) is $2P_{LZ}(1-P_{LZ})$ since two traversals of the crossing point occur.

Details of the $^1B_2/^1A_1$ crossing point used in the LZ calculation are presented in Fig. 7 as well as the numerical values extracted from the *ab initio* curves. The LZ results on the $^1A_1/^1B_2$ state interactions in the $Zn\cdot N_2$ system indicate a hopping probability of 0.068. This represents a 7% chance of direct deactivation to the ground state from the bound state initially accessed in absorption.

b. Singlet/triplet crossings LZ calculations were also undertaken for the spin singlet/triplet crossings evident in Fig. 3 between the $^1B_2/^3A_1$ states and the $^1B_2/^3B_1$ states. The matrix elements of these spin–orbit induced couplings are listed in Appendix B. Using the one-dimensional LZ method outlined above, hopping probabilities of 1.0% and 1.2% were obtained for the $^1B_2/^3B_1$ and $^1B_2/^3A_1$ state crossings, respectively. Both of these are almost an order of magnitude less than vibronically induced singlet $^1B_2/^1A_1$ state crossings.

It is evident in Fig. 4 that a singlet/triplet curve crossing occurs also in the collinear approach between the repulsive $^3\Sigma_1$ state and the bound $^1\Pi_1$ state on its attractive wing. The matrix element for this $^1\Pi_1/^3\Sigma_1$ state crossing is listed as $V_{12}=\zeta/2$ in Appendix B. Using the procedure outlined above the hopping probability of this spin–orbit induced coupling is found to be 0.026.

IV. DISCUSSION

A. Absorption spectra

The threefold splitting present on the absorption band of atomic zinc in solid nitrogen has also been observed in the excitation spectra recorded[11] for atomic zinc isolated in the solid rare gas hosts Ar, Kr, and Xe. This splitting has been assigned to dynamic Jahn-Teller coupling in the degenerate excited state. For the Jahn-Teller modes to be active, the zinc atom must be isolated in a highly symmetrical site in the ground electronic state with a symmetry lowering in the excited electronic state arising from coupling to noncubic electron–phonon modes. With the availability of the van der Waals radii of metal atoms with rare gas partners from spectroscopic data, identification of substitutional site occupancy of zinc in the solid rare gases Ar, Kr, and Xe has been made. For example, the $Zn\cdot Kr$ ground $X\,^1\Sigma_0^+$ state bond length is known to be 4.2 Å and since the substitutional site diameter of solid krypton[36] is 3.99 Å, the zinc atom resides easily in a single substitutional site of the Kr matrix. Unfortunately such information does not exist on the equivalent $Zn\cdot N_2$ 1:1 complex,[37] but based on the behavior of other metal atom/rare gas systems it is expected that the ground state bond length will be around 4 Å. Given that the substitutional site diameter in solid nitrogen is 3.95 Å, it is expected that atomic zinc will occupy this site as inferred in the Hg/N_2 system.[38]

TABLE I. Mulliken population analysis performed at the SCF level for the bound $^1B_2$ electronic states of ZnN_2 in side-on geometry. The *z*-axis has been chosen as the main axis in the coordinate system used. For the nitrogen atoms only $2s$ and $2p$ type electrons are considered, while for the zinc atom only the $3d$, $4s$, and $4p$ valence subshells are included. The total population on each atom is given in the column on the extreme right.

	S	p_x	p_y	p_z	$d_{x^2-y^2}$	d_{z^2}	d_{xy}	d_{xz}	d_{yz}	Total
Zn	1.061	0.034	0.262	0.257	~2	~2	~2	~2	~2	11.636
N1	1.750	0.98	1.181	1.271	⋯	⋯	⋯	⋯	⋯	5.182
N2	1.750	0.98	1.181	1.271	⋯	⋯	⋯	⋯	⋯	5.182

On the basis of substitutional site occupancy, optical absorption from the ground electronic state of the $Zn(^1S_0)\cdot N_2$ complex will initially reach the neutral $Zn(^1P_1)\cdot N_2$ curve since the charge transfer state is accessed at distances less than 2.62 Å. This expectation is consistent with the observation of only a small (785 cm^{-1}) shift of the resonance transition in solid nitrogen (210 nm) from the gas phase value of 213.9 nm.

B. Charge transfer contributions

Mulliken populations analyses of the lowest energy levels found in the two approach symmetries were conducted at the SCF level for the extent of the charge transfer in excited state stabilisations. The results for the side-on approach, collected in Table I, indicate the charge deficit on the zinc atom is $\delta=+0.364$ while the charge surplus on each of the nitrogen atoms is $\delta=-0.182$. This behavior is consistent with the simple Coulombic model presented earlier for the contribution of charge-transfer interactions in the binding of excited states. The main changes in charge distribution identified in the population analysis are related to the metal–ligand bonding character of the $4a_1$ and $3b_2$ molecular orbitals. The $4a_1$ orbital contains an important interaction between the π_z orbital of N_2 and the $s-p_z$ combination of the metallic orbitals (the *z*-axis is chosen as the main axis), while the $3b_2$ orbital is mainly formed as a contribution of the π_z^* orbital of the ligand and the zinc p_y-type orbital.

Mulliken population analysis of the $^1\Pi_y$ electronic states of the linear approach also point toward a charge transfer from the metal to the nitrogen molecule. As indicated in Table II by the partial charges of $\delta=+0.422$ on the Zn atom and $\delta=-0.546$ on N1 and $\delta=+0.124$ on N2. In fact, the

TABLE II. Mulliken population analysis for the bound $^1\Pi_x$ state of ZnN_2 at the SCF level. As for the side-on coordination mode, the analysis includes only the $2s$ and $2p$ type electrons of the nitrogen atoms—for the zinc atom only the subshells $3d$, $4s$, and $4p$ are included in the valence region.

	S	p_x	p_y	p_z	$d_{x^2-y^2}$	d_{z^2}	d_{xy}	d_{xz}	d_{yz}	Total
Zn	0.983	0.018	0.383	0.198	~2	~2	~2	~2	~2	11.578
N1	1.559	1.235	1.324	1.427	⋯	⋯	⋯	⋯	⋯	5.546
N2	1.556	0.765	1.276	1.279	⋯	⋯	⋯	⋯	⋯	4.876

main changes in the total population of the zinc atom basis functions, i.e., the decrease of the p_y type-function and the small increase of the p_z type-function, suggest a bond picture in accordance with the Chatt–Duncanson[39] model. In this model the ligand acts as an electron donor through a sigma-type interaction (in this case the interaction between the originally empty p_z orbital of the zinc atom with the doubly occupied σ-type orbital of the N_2 molecule formed from the $p_z(N_1)-p_z(N_2)$ combination). This is accompanied by a π-type backbonding donation from the metallic atom toward the ligand (in the $Zn\cdot N_2$ case, the interaction among the originally single occupied p_y type orbital from the zinc atom and the empty π_y^* of the nitrogen molecule).

C. Surface crossings

From the calculated potential energy curves shown in Fig. 3, it is clear that in the excited state relaxation, there should be competition to form the ground state zinc atom through $^1A_1/^1B_2$ interaction, and to form the triplet Zn atom through $^3A_1/^1B_2$ or $^3B_1/^1B_2$ spin–orbit induced reaction. The efficiencies of these processes have been investigated in the one-dimensional LZ calculations and the singlet interaction is found, as expected, to be the more efficient. The singlet/triplet interactions are approximately an order of magnitude smaller. This difference can be rationalized since the latter two couplings depend largely on the spin–orbit coupling of atomic zinc which is relatively small, while the singlet coupling is merely vibration-induced. However, in spite of the very different efficiencies of these couplings, sight should not be lost of the singlet/triplet crossings. Thus, in the gas-phase any $^1B_2$ which survives the first crossing of $^1A_1$ with $^1B_2$ can possibly come back up the potential curve and cross to the $^3B_1$ or $^3A_1$ curve with outgoing momentum, to produce ^3P_J atoms. This would correspond to the small, but significant (6 Å^2) branching cross section leading to the triplet.

Under matrix conditions rapid deactivation to the bottom of the $^1B_2$ well occurs, minimizing the contribution of singlet/triplet curve crossing. It should however, be kept in mind that the singlet/triplet curve crossings occur, as shown in Fig. 3, prior to the singlet/singlet crossing. Thus a small but finite amount of triplet atomic zinc should be produced also under matrix conditions. However, as reported triplet emission is not observed with singlet excitation. Moreover, even with direct laser excitation of the triplet state no emission is observed. This would suggest that the triplet emission is also completely quenched in the matrix, despite the small gas phase quenching cross section of 0.6 Å^2 for the $Zn(^3P)$ by nitrogen. From the excited state curves calculated in this study, this quenching must occur from crossing of the bound $^3B_2$ curve and the repulsive $^1A_1$ curve.

V. CONCLUSIONS

Complete fluorescence quenching has been observed for the first excited singlet state of atomic zinc in nitrogen matrices. The mechanism of the corresponding $E-V$ energy transfer process has been identified in quantum mechanical calculations as due to a low energy crossing of the bound excited singlet state and the repulsive ground singlet state (singlet crossing) present in the side-on approach geometry. The bound nature of the excited states in this and the end-on mode approaches calculated is related to a significant charge transfer contribution to the binding. Consistent with simple energetics arguments, population analysis points towards a charge transfer from the metal atom to the nitrogen molecule. The absence of similar low energy crossings in the end-on approach point to a less important role for this configuration in the quenching process under matrix-isolation conditions. Hence, we conclude that the excited singlet state quenching of atomic zinc by molecular nitrogen occurs predominately for side-on approach of these two species. Other crossings identified in the side-on approach involve states of different spin. The interaction between the spin singlet states at their crossing is found, from Landau–Zener calculations, to be the more efficient. This can be rationalized since it is vibronically-induced while the interaction of the different spin states depends mostly on the spin–orbit coupling of atomic Zn which is relatively small.

ACKNOWLEDGMENTS

We would like to acknowledge P. Gürtler, B. Healy, and S. Petersen for technical assistance in the recording of the experimental data. Fruitful discussions with Professor Bill Breckenridge on the surface hopping model were significant in the development of this work. This research was funded by the European Union TMR 1999-2001 ''Access to Large Scale Facilities'' Program. One of us (F.C.) acknowledges the hospitality of the Centro de Investigaciones Teoricas de la FES Cuatitlan de la UNAM, during his sabbatical leave.

APPENDIX A: MATRIX ELEMENTS FOR THE VIBRONICALLY COUPLED SINGLET $^1B_2/^1A_1$ STATES

To determine the strength of the interaction between the singlet $^1B_2(^1P_1)$ and $^1A_1(^1S_0)$ states, we have taken the calculated diabatic curves, then estimated the vibrational coupling matrix elements as the $^1B_2$ state distorts when undergoing an antisymmetric stretch vibration. In the calculations, done near the $^1B_2$ state minimum, this is realised by rotating the N_2 molecule around its center-of-mass in the plane of the triatomic $Zn\cdot N_2$ system. The idea is that the direct product of the B_2 symmetry, asymmetric stretch vibrational mode with the B_2 symmetry electronic state gives a state of total symmetry A_1. This is identical to the symmetry of the vibrationless $^1A_1$ potential curve, hence a curve avoidance is induced between the two states.

APPENDIX B: MATRIX ELEMENTS FOR SPIN–ORBIT COUPLED $^1B_2(^1P_1)$ AND $^3A_1(^3P_1)$ STATES

The matrix element, V_{12}^2, coupling two potentials, 1 and 2, is derived from the spin–orbit coupling term whose magnitude depends first, on the metal atom considered and second, on the spatial symmetries of the interacting states. The coupling term for the $^1\Pi_1/^3\Sigma_1$ states of the collinear $Zn\cdot N_2$ system[40,41] is one-half the spin–orbit coupling constant of the free atom, $V_{12}=\zeta/2$. For the $^1B_2/^3A_1$ states[41] of the $Zn\cdot N_2$ system in C_{2v} symmetry, $V_{12}=\sqrt{2}\zeta/4$. The spin–orbit coupling constant, ζ, of the $4s4p$ configuration of atomic zinc is $\zeta_{4p}=2(E_{^3P_2}-E_{^3P_0})/3$ which from Moore's Tables has a value of 386.0 cm^{-1}. It should be kept in mind that the use of the atomic spin–orbit coupling constant is valid only when the $4p$ orbital is undistorted. As this may not be the case in the charge transfer state, the LZ hopping probabilities should only be taken as first estimates. .

[1] W. H. Breckenridge, Acc. Chem. Res. **22**, 21 (1989).
[2] C. Crepin, F. Legay, N. Legay-Sommaire, and A. Tramer, Chem. Phys. **136**, 1 (1989).
[3] N. Legay-Sommaire and F. Legay, J. Phys. Chem. **99**, 16951 (1995).
[4] C. Crepin and P. Millie, Chem. Phys. **133**, 377 (1989).
[5] M. Czajkowski, E. Walentynowicz, and L. Krause, J. Quant. Spectrosc. Radiat. Transf. **28**, 493 (1982).
[6] W. H. Breckenridge and A. M. Renlund, J. Phys. Chem. **83**, 1145 (1979).
[7] H. Umemoto and K. Matsumoto, Chem. Phys. Lett. **236**, 408 (1995).
[8] W. W. Duley, Proc. Phys. Soc. London **91**, 976 (1967); Nature (London) **210**, 264 (1966).
[9] S. L. Laursen and H. E. Cartland, J. Chem. Phys. **95**, 4751 (1991).
[10] B. Hoffmann-Millack, A. Klein, H. Lagier, B. Maid, and J. Hormes, Chem. Phys. **136**, 453 (1989).
[11] V. A. Bracken, P. Gürtler, and J. G. McCaffrey, J. Chem. Phys. **107**, 5290 (1997).
[12] W. Schroeder, H. Wiggenhauser, W. Schrittenlacher, and D. M. Kolb, J. Chem. Phys. **86**, 1147 (1987).
[13] I. Wallace, R. R. Bennett, and W. H. Breckenridge, Chem. Phys. Lett. **153**, 127 (1988).
[14] R. R. Bennett and W. H. Breckenridge, J. Chem. Phys. **92**, 1588 (1990).
[15] I. Wallace, J. G. Kaup, and W. H. Breckenridge, J. Phys. Chem. **95**, 8060 (1991).
[16] I. Wallace, J. Ryter, and W. H. Breckenridge, J. Chem. Phys. **96**, 136 (1992).
[17] R. R. Bennett and W. H. Breckenridge, J. Chem. Phys. **96**, 882 (1992).
[18] H. Umemoto, T. Ohnuma, H. Ikeda, S. Tsunashima, K. Kuwahara, F. Misaizu, and K. Fuke, J. Chem. Phys. **97**, 3282 (1992).
[19] S. Martrenchard-Barra, C. Jouvet, C. Lardeux-Dedonder, and D. Solgadi, J. Chem. Phys. **98**, 5281 (1993).
[20] O. Roncero, J. Beswick, N. Halberstadt, and B. Soep, in *Dynamics of Polyatomic van der Waals Complexes* (Plenum, New York, 1990), Vol. 227; also, A. Bastida, J. Requena, B. Soep, N. Halberstadt, and J. Beswick, J. Chim. Phys. (Paris) **92**, 384 (1995).
[21] W. H. Breckenridge, M. D. Morse, and J. G. McCaffrey, J. Chem. Phys. **109**, 3137 (1998).
[22] C. E. Moore, *Atomic Energy Levels* (U.S. GPO, Washington, D.C., 1952).
[23] The PSHF pseudopotential is an adaptation made by J. P. Daudey of the HONDO code written by M. Dupuis, J. Rys, and H. F. King, Theor. QCPE program 338 (1977).
[24] Ph. Durand and J. C. Barthelat, Theor. Chim. Acta **38**, 283 (1975); J. C. Barthelat, Ph. Durand, and A. Serafini, Mol. Phys. **33**, 179 (1977); J. C. Barthelat, Ph. Durand, and A. Serafini, Gazz. Chim. Ital. **108**, 225 (1978); M. Pélissier and Ph. Durand, Theor. Chim. Acta **55**, 43 (1980).
[25] M. M. Hurley, L. F. Pacios, P. A. Christiansen, R. B. Ross, and W. C. Ermler, J. Chem. Phys. **84**, 6840 (1986).
[26] A. J. H. Wachters, J. Chem. Phys. **52**, 1033 (1970).
[27] L. F. Pacios and P. A. Christiansen, J. Chem. Phys. **82**, 2664 (1985).
[28] L. F. Pacios and P. C. Gomez, Int. J. Quantum Chem. **49**, 817 (1994).
[29] For these calculations the GMCP program was used. This program was written by R. Carbó, M. Pélissier, J. P. Daudey, and J. Rubio and it is based on the Elementary Jacobi Rotation algorithm.
[30] B. Huron, P. Rancurel, and J. P. Malrieu, J. Chem. Phys. **58**, 5745 (1973).
[31] S. Evangelisti, J. P. Daudey, and J. P. Malrieu, Chem. Phys. **75**, 91 (1983).
[32] P. J. Hay, T. H. Dunning, and R. C. Raffenetti, J. Chem. Phys. **65**, 2679 (1976).
[33] The splitting on the higher energy band is thought to be due to the removal of the Π state degeneracy by the symmetry of the site accommodating the zinc dimer molecule.
[34] It will be noted in Fig. 4 that a $^1\Pi_1/^1\Sigma_0$ crossing does occur in the end-on approach, but at high energy on the inner wall of the $^1\Pi_1$ state.
[35] H. Eyring, J. Walter, and G. E. Kimball, *Quantum Chemistry* (Wiley, New York, 1944), pp. 326–329.
[36] C. Kittel, *Introduction to Solid State Physics*, 6th ed. (Wiley, New York, 1986), p. 58.
[37] It is expected that the geometry is T-shaped.
[38] F. Legay, N. Legay-Sommaire, and V. Chandrasekharan, J. Phys. Chem. **94**, 8548 (1990).
[39] J. Chatt and L. A. Duncanson, J. Chem. Soc. **1953**, 2939; also M. J. S. Dewar, Bull. Soc. Chim. Belg. **71**, 18 (1951).
[40] H. Lefebvre-Brion and R. W. Field, *Perturbations in the Spectra of Diatomic Molecules* (Academic, New York, 1986), Chap. 6.
[41] S. Bililign, M. D. Morse, and W. H. Breckenridge, J. Chem. Phys. **98**, 2115 (1993).